

## Dislocation Analysis of Thermal-Cycle-Annealed Mesa-Structured HgCdTe/HgTe/CdTe/ZnTe/Si (211)

M. Vaghayenagar<sup>1</sup>, S. Simingalam<sup>2</sup>, Y. P. Chen<sup>2</sup> and D. J. Smith<sup>3</sup>

<sup>1</sup>. School for Engineering of Matter, Transport and Energy, Arizona State University, Tempe, AZ 85287

<sup>2</sup>. Army Research Laboratory, 2800 Power Mill Rd, Adelphi, MD 20783

<sup>3</sup>. Department of Physics, Arizona State University, Tempe, AZ 85287

Due to its band-gap tunability,  $\text{Hg}_x\text{Cd}_{1-x}\text{Te}$  (MCT), has been the dominant material for infrared (IR) focal-plane-array (FPA) technology [1]. The emergence of a new generation of IR detectors has pushed the substitution of Si for traditional CdZnTe substrates. Although cheaper and larger in size, the growth of high quality MCT on Si has been hindered by the high dislocation density induced by the large lattice mismatch (19.5%) between Si and MCT, which will deteriorate the device performance due to inoperable pixels in detector arrays [2,3]. The combination of plasma processing for production of novel mesa structures with relatively flat side-wall and post-growth annealing, has recently been proposed as an effective approach for reduction of dislocation density [4]. Long-wave length MCT layer,  $x=0.22$ , was grown by molecular beam epitaxy on  $2 \times 2 \text{ cm}^2$  composite (211) substrates consisting of thin ( $\sim 15 \text{ nm}$ ) ZnTe and thick ( $\sim 10 \mu\text{m}$ ) CdTe buffer layers. Plasma processing was implemented to etch mesa-bars along certain crystallographic directions. Post-etch annealing was carried out repeatedly four times with a slow ramp to  $250^\circ\text{C}$  followed by 2min ramp from  $250^\circ\text{C}$  to  $400^\circ\text{C}$ , holding 5min at  $400^\circ\text{C}$ , 20 min radiative cool to  $250^\circ\text{C}$ , and finally radiative cool to room temperature. Finally, Schaaque's etchant was used to decorate the sample surface with pits. These samples were investigated to determine the effectiveness of the mesa structure and post-annealing to reduce the dislocation density. FIB was used to prepare  $\langle 110 \rangle$  XTEM samples along the edge and the center of the mesa bars. Cross-section samples were studied using bright-field two-beam TEM, using Philips-FEI CM200-FEG.

Figure 1(a) shows low mag SEM image of the mesa structure, and the area where the samples were lifted out is marked with a circle. Figures 1(b, c) show the mesa center decorated with pits, coded as #1 through #5, and corresponding lift-out sample. A series of **g.b** analysis,  $\pm\{(-11-1), (-1-11), (0-22), (31-1), \text{ and } (-400)\}$  were done to determine Burgers vector of MCT dislocations. Figures 2(a-d) show two-beam images with the dislocation segments going in and out of contrast. Figures 3(a, b) show the mesa edge decorated with pits, coded as #1 through #4, and corresponding lift-out sample. A similar **g.b** analysis were done to determine Burgers vector of dislocations near the mesa wall. Figures 4(a-d) show selected 2-beam images of the dislocation segments. These defects are being analyzed using  $\langle 011 \rangle$  stereographic projection to determine dislocation type, dislocation line, slip plane and mobility of these segments. These results will be presented at the meeting.

### References:

[1] A. Rogalski, *Infrared. Phys. Techn.* **43** (2002), 187-210.

[2] A. Rogalski, *Infrared. Phys. Techn.* **50** (2007), 240-252.

[3] R. N. Jacobs et al., *J. Electron. Mater.* **42** (2013), 3148-3155.

[4] A. J. Stoltz et al., *J. Electron. Mater.* **40** (2011), 1785-1789.

[5] This work was supported by Army Research Office Grant #63749-EL. We gratefully acknowledge the use of facilities within the John M. Cowley Center for HREM at Arizona State University.

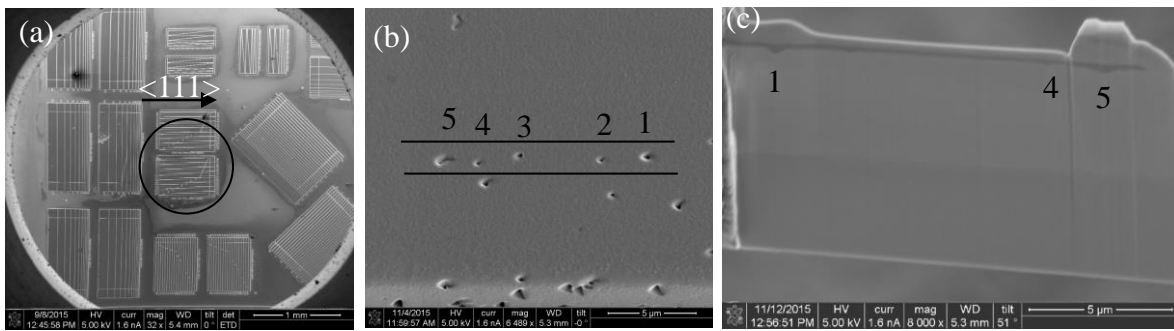


**Figure 1.** SEM images: (a) Low-mag image of Mesa-structures; (b) selected series of pits along the center of mesa for lift-out; and (c) the lift-out sample.

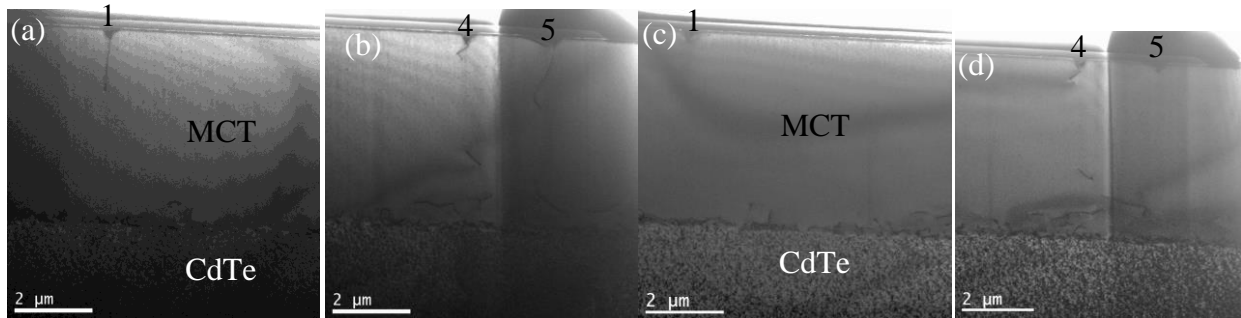


**Figure 2.** XTEM images: (a, b) for  $\pm (0-22)$  condition, and (c, d) for  $\pm (11-1)$  condition.

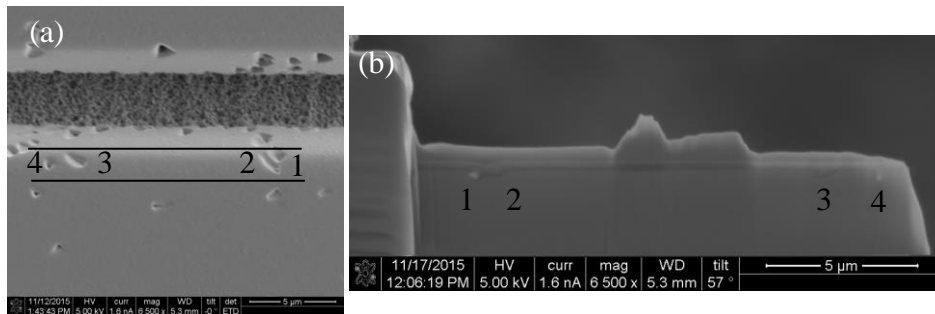


**Figure 3.** SEM images: (a) series of pits along the wall of mesa for lift-out; and (b) corresponding lift-out sample.

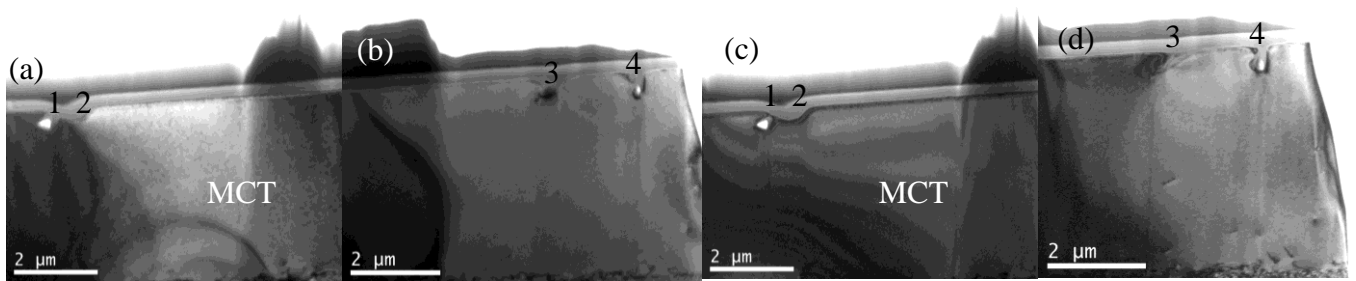


**Figure 4.** XTEM images: (a, b) for  $\pm (400)$  condition; and (c, d) for  $\pm (11-1)$  condition.